Broadband Enhancement in the Spectral Response of Photovoltaic Modules with Flower-like Silver Particles

Yan Wang , Feng Zhang , Xinmin Fan * , Yabin Lu , Chunyan Wang , Xiaodong Huang , Lujun Zhang

Posted Date: 20 July 2023

doi: 10.20944/preprints202307.1401.v1

Keywords: broadband enhancement; photovoltaic; flower-like silver particles

Article

Broadband Enhancement in the Spectral Response of Photovoltaic Modules with Flower-like Silver Particles

Yan Wang [1], Feng Zhang [2], Xinmin Fan [1,*], Yabin Lu [2], Chunyan Wang [1], Xiaodong Huang [1] and Lujun Zhang [1,*]

[1] Department of Physics and Optoelectronic Engineering, Weifang University, Weifang 261061, China
[2] Institute of Modern Optics, College of Electronic Information and Optical Engineering, Nankai University, Tianjin 300350, China
* Correspondence: xinminfan@163.com (X.F.); zhang_lujun1985@163.com (L.Z.)

Abstract: Recent researches have indicated that metal nanoparticles, known for their unique optical properties, can enhance the spectral response of photovoltaic modules. Since most nanoparticles demonstrate enhancement effects within a specific wavelength range, broadening the spectral response of photovoltaic modules is critical for their application in imaging, energy harvesting, and optical communication. In this study, we applied flower-like silver particles to achieve this broadband enhancement. The optical absorption of photovoltaic modules, featuring an amorphous Si p-i-n structure, was improved across a broad wavelength range of 400~2000 nm by integrating these flower-like silver particles, resulting in an approximately tenfold increase in peak spectral responsivity. Theoretical investigation further elaborates that the enhancement originates from the near-field effects of silver particles due to the interaction of different parts of the flower-like silver particles. Through these studies, we demonstrate that, utilizing the subwavelength silver particles with roughness surface can achieve the spectral response of the photovoltaic modules enhanced in broadband range, which can improve the utilization efficiency of optical energy for the applications of sensing, imaging, optical communication, and energy harvesting.

Keywords: broadband enhancement; photovoltaic; flower-like silver particles

1. Introduction

Due to their low cost and ease of fabrication, semiconductor photovoltaic modules have found widespread applications in both military and civilian industries [1–3]. A photodetector possessing a broadband spectral response holds significant implications for sensing, imaging, optical communication, and energy harvesting [4–8]. Therefore, developing a photodetector with a broadband spectral response has become a primary research area. Significant efforts have been directed towards improving the spectral response by modifying the material and structure of photovoltaic modules [9–11]. Over the past decade, with the advancement of plasmonic, enhancing the performance of photodetectors through the exploitation of metal nanostructures has been considered viable [12–16]. For instance, Naomi J. Halas and colleagues achieved enhanced spectral response in a photodiode within the range of 1250~1650 nm by using a gold (Au) antenna [17]. A substantial increase in the photoconductivity of amorphous silicon was also reported through the use of silica-coated gold nanorods [18]. Our previous work systematically explored the fabrication and optical properties of flower-like silver nanoparticles. In our findings, we observed that these nanoparticles, characterized by their rough morphological features, exhibited broadband plasmon resonance peaks spanning across the visible and near-infrared regions of the spectra. Moreover, due to these specific characteristics of the flower-like silver nanoparticles, we achieved enhanced Surface-Enhanced Raman Scattering (SERS) intensity [19]. These results inspired us to design a nanoparticle-coupled semiconductor with the objective of achieving enhanced response over a broad spectral

Preprints (www.preprints.org) | NOT PEER-REVIEWED | Posted: 20 July 2023 doi:10.20944/preprints202307.1401.v1

range. By providing this brief yet comprehensive summary of our previous work, we aim to give reviewers a clearer understanding of the basis and the objectives of our current study.

In this paper, we successfully fabricated an amorphous silicon (a-Si) photovoltaic module embedded with flower-like silver particles. We measured the transmittance, reflectance, and absorption characteristics of the spectra, with a particular focus on the spectral responses of the photovoltaic modules both with and without silver particles. Our findings show that, compared to modules without silver particles, the ones with silver particles demonstrate enhanced absorption and response across a broadband spectral range, extending from the visible to the near-infrared region. Furthermore, we examined the near-field optical properties of the flower-like silver particles with an average diameter of 500 nm. The results revealed that the interaction induced by the rough surface of the different components of the silver particles provides the flower-like silver particle with a unique field enhancement capability in the broadband range. This feature plays a pivotal role in the broadband enhancement of spectral response for the photovoltaic structure.

2. Materials and Methods

2.1. Preparation of flower-like silver particles

Flower-like silver particles were synthesized using the standard chemical reduction method of silver nitrate, as reported in the existing literature [20,21]. All starting materials were of reagent grade and used as received, unless specified otherwise.

We added 0.6 ml of 1 M $AgNO_3$ and 6 ml of 100 mM polyvinylpyrrolidone aqueous solutions to 30 ml of deionized water. The mixture was stirred continuously at room temperature, after which 0.6 ml of 1 M ascorbic acid was rapidly introduced. The stirring continued until no further color change was observed. Following a centrifugation at 4000 rpm for 15 minutes, the flower-like silver particles were obtained.

2.2. Optical modeling

Building upon our previous work, the flower-like silver particles consist of two components. One is the core particle, approximately 400 nm in size, and the other consists of surface protrusions, each around 100 nm in size. This design ensures that the total size of the particle is 500 nm [19], as illustrated in Figure 1.

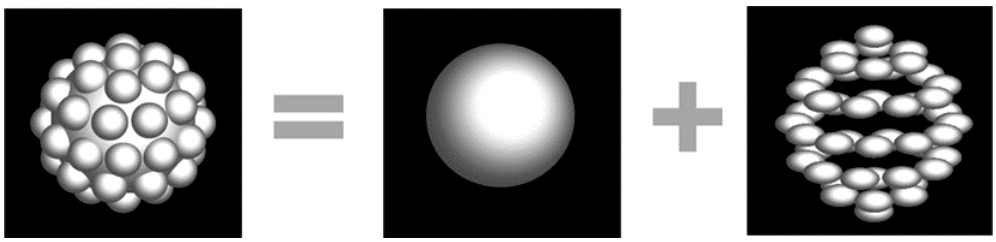

Figure 1. Schematic diagrams of flower-like silver particles.

The surface local fields of the silver particles were calculated using the three-dimensional finite difference time domain (FDTD) method. The dielectric data for silver were adopted from Palik [19,22]. A perfectly matched layer (PML) was employed as the boundary condition. The excitation light was set to be incident in the positive z-direction and polarized along the x-axis.

2.3. Instrumentation

Scanning electron microscopy (SEM) images of the specimens were acquired with a JEOL JSM-6700f scanning electron microscope at 3.0 kV. The transmittance and reflectance spectra were recorded using a Cary500 UV-visible-infrared absorption spectrometer. The photocurrent was assessed with a Keithley 6430 digital source meter.

Preprints (www.preprints.org) | NOT PEER-REVIEWED | Posted: 20 July 2023 doi:10.20944/preprints202307.1401.v1

3. Results and Discussion

The flower-like silver particles were deposited onto the surface of an a-Si p-i-n structure, which was immobilized on ITO glass, and then left to dry naturally in a nitrogen environment. As shown in Figure 2(a), the thickness of the a-Si p-i-n structure is measured to be 500 nm. From the SEM image shown in Figure 2(b), it can be observed that the silver particles, with an average diameter of ~500 nm, are distributed randomly on the surface of the a-Si p-i-n structure.

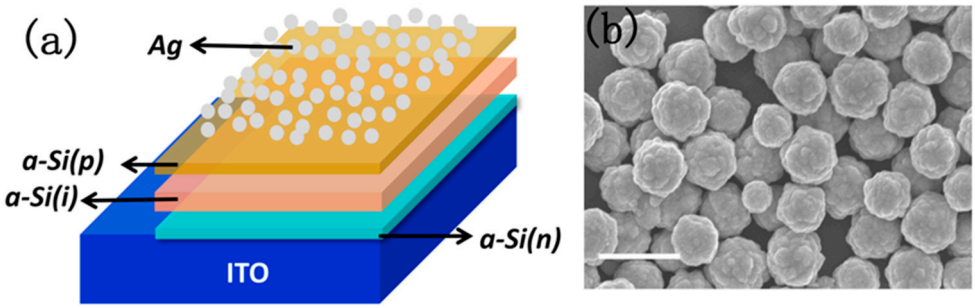

Figure 2. (a) Schematic of the a-Si p-i-n photovoltaic structure with silver particles on the surface. (b) The SEM image of the flower-like silver particles on the surface (the scale bar= 1μm).

The transmittance (Figure 3(a)) and reflectance (Figure 3(b)) of the a-Si p-i-n photovoltaic structure, both with and without silver particles, were respectively measured using the diffuse reflection method. Absorptance, defined as Abs (%) =1-R (%)-T (%), is depicted in Figure 3(c). For the sample adorned with silver particles, a decrease in transmittance is noted across the wavelength range of 450~2000 nm, particularly between 450 nm and 1600 nm. As for reflectance, it decreased across the full wavelength range of 200~2000 nm when silver particles were present on the photovoltaic structure. Hence, absorptance was enhanced across the entire wavelength spectrum, from 200 nm to 2000 nm. A comparison of the spectral curves of the a-Si p-i-n structure with and without silver particles reveals no change in the shape of absorption. This phenomenon is attributed to the flower-like silver particles possessing broadband plasmon resonance peaks in the visible and near-infrared regions of the spectra, thereby enhancing absorption across the entire wavelength range for the photovoltaic module. A comparison of the spectra of the semiconductor with and without flower-like silver particles demonstrates that the spectral response of the a-Si p-i-n structure can be enhanced through the incorporation of flower-like silver particles.

Then, the photocurrent in the wavelength range of 400~800nm of the a-Si p-i-n photovoltaic structure with and without silver particles was further measured, respectively. The responsivity was calculated by $R = I_L/P_{inc}$, where R is defined as the responsivity, I_L is the photocurrent, and P_{inc} is the power of the incident light. We plotted the responsivity R as a function of wavelength, as shown in Figure 4. The results show that the structure without silver particles has the spectral response at the wavelength range of 400nm to 800nm, which is consistent with the results at the previous report [23]. Compared to the structure without silver particles, the spectral response of the composite structure has been obviously enhanced. Especially, at the wavelength of 650 nm, i.e., at the peak of the responsivity, the responsivity was enhanced by about 10 times. At the same time, the spectral response shape was consistent with that of the structure without silver particles.

Preprints (www.preprints.org) | NOT PEER-REVIEWED | Posted: 20 July 2023 doi:10.20944/preprints202307.1401.v1

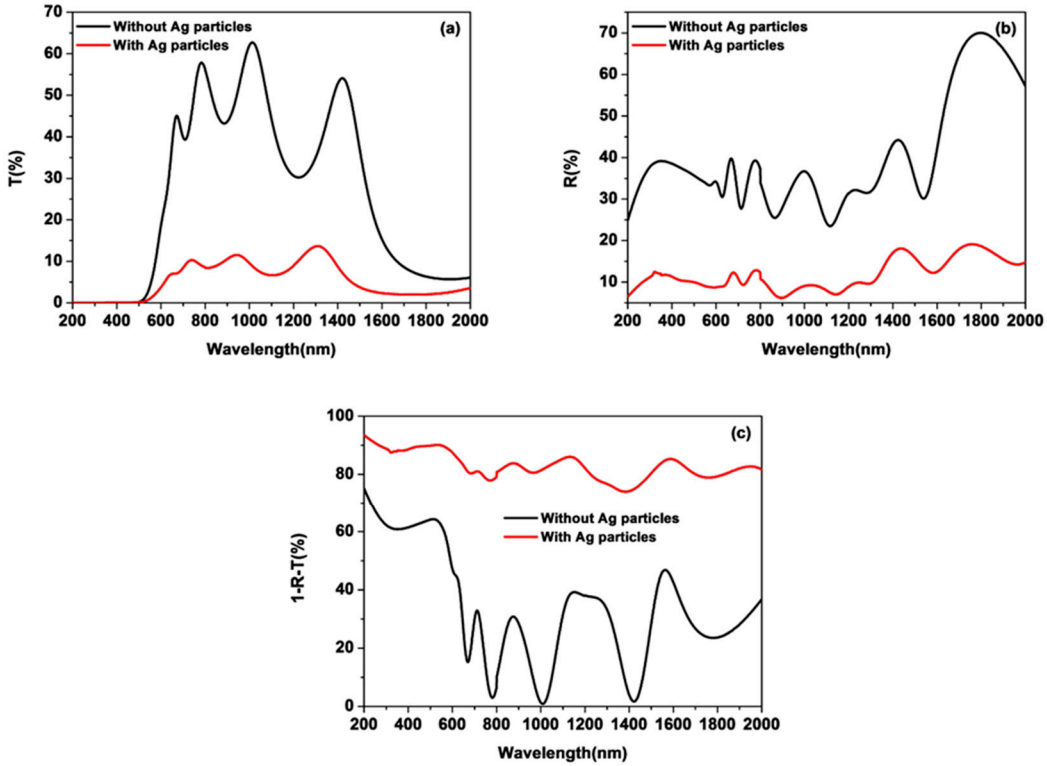

Figure 3. The spectra measured for (a) the transmittance, (b) the reflectance, and (c) the absorptance, respectively.

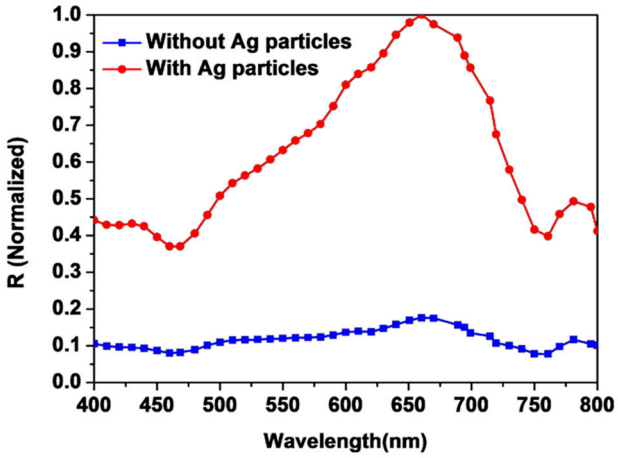

Figure 4. The responsivity of the a-Si p-i-n structure with and without silver particles, respectively.

For a semiconductor, the responsivity $R_{\lambda,I}$ is proportional to the intensity of the radiation field and can be expressed as

$$R_{\lambda,I} \propto C\left|\vec{E}\right|^2 \quad (1)$$

where the parameter C represents a constant. Consequently, an increase in the intensity of the radiation field leads to an enhancement of the spectral response. In our photovoltaic structure with silver particles, the incident light initially interacts with the flower-like silver particles deposited on the surface of the a-Si p-i-n structure, stimulating the localized surface plasmon resonance of the silver particles and enhancing the field around them. This interaction consequently amplifies the intensity of the radiation field of the semiconductor.

Preprints (www.preprints.org) | NOT PEER-REVIEWED | Posted: 20 July 2023 doi:10.20944/preprints202307.1401.v1

The results shown in Figure 3 demonstrate that the flower-like silver particles, with an average diameter of 500 nm, can enhance the spectral response across the full wavelength range of 400~800nm. This suggests that the flower-like silver particles possess a distinctive field enhancement capability within the 400~800 nm wavelength range. Therefore, it is believed that the surface roughness structure of the flower-like silver particle plays a pivotal role in contributing to field enhancement.

To further investigate the influence of the surface protrusions, the flower-like silver particle was considered to comprise two components: a large core particle of ~400 nm in size, and smaller surface particles of ~100 nm, as shown in Figure 1. The plasmon resonance mode for the surface particles maintains the form of a dipole consistently across the 400 nm to 800 nm wavelength range. However, for the core particle, the plasmon resonance mode starts as a multipole at short wavelengths, transitioning to a dipole at longer wavelengths [24].

The FDTD method was subsequently utilized to study the interaction between the core particle and the surface particles at wavelengths of 410 nm and 650 nm, respectively. Figure 5 depicts the local field of three neighboring surface particles stimulated by the local field of the core particle. Under the 410 nm radiation, the strongest field for the surface particles occurs in the gap of the surface roughness structure, as depicted in Figure 5(a). Under 650 nm wavelength radiation, the electric field of surface particles is concentrated on the outer area of the surface, as presented in Figure 5(b). These simulation results disclose that the effects of the core particle on the surface particles differ in the short and long wavelength ranges, and the "hot spot" of the surface particles also varies accordingly. Furthermore, the interaction between surface particles was also examined. It is found that the electron distribution of the surface particles is determined by the core particle, considered as a whole.

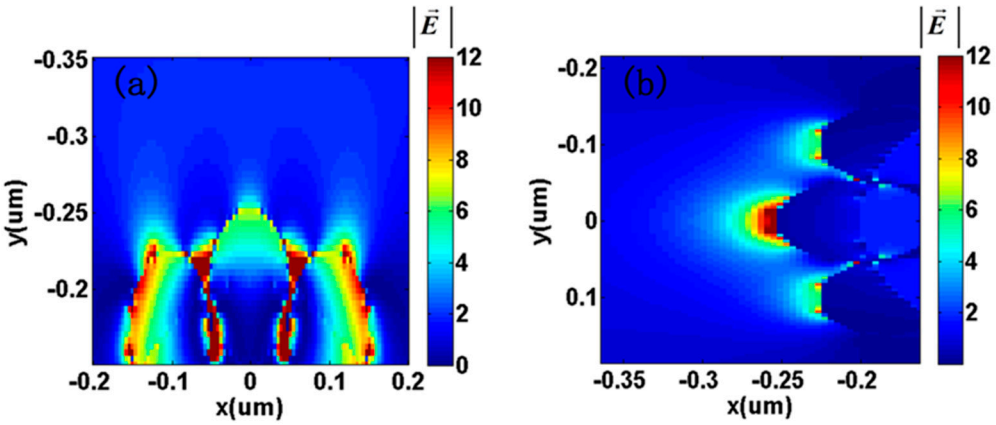

Figure 5. The distribution of electric field around three neighboring surface particles excited by the local field of the core particle. (a) at the wavelength of 410 nm, (b) at the wavelength of 650 nm.

For a single surface particle, the resonance model is solely a dipole in the wavelength range of 400~800 nm, and can therefore be considered as a dipole. Under the radiation at a wavelength of 410 nm, the resonance model of the core particle is multipole. The internal electron oscillations are not just parallel but also perpendicular to the polarization of the incident light. As a result, for neighboring particles in the "Shoulder to Shoulder" pattern (the axis of which is parallel to the polarization of the incident light) of the surface particles, interaction between electrons can occur [25,26], as illustrated in Figure 6(a). The strongest electric field occurs in the gap between the two particles which are in the "Shoulder to Shoulder" pattern.

Under radiation at a wavelength of 650 nm, the resonance model of the core particle is a dipole, and collective electron oscillations are parallel to the direction of the incident light. The internal electrons concentrate on both sides of the core particle. Therefore, the interaction of surface particles in the "Shoulder to Shoulder" pattern is suppressed. Conversely, for neighboring particles in the "Head-to-Head" pattern (the axis of which is perpendicular to the polarization of the incident light) among the surface particles, the local field is enhanced under the action of the core particle, as depicted in Figure 6(b). In this case, the electric field is concentrated in the outer area.

Preprints (www.preprints.org) | NOT PEER-REVIEWED | Posted: 20 July 2023 doi:10.20944/preprints202307.1401.v1

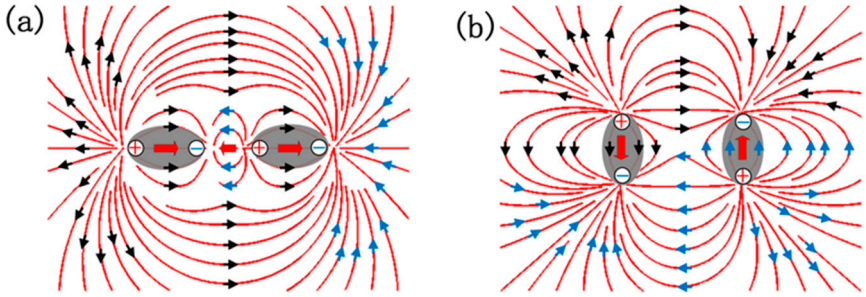

Figure 6. A sketch of the electric field distribution of two neighboring surface particles. (a) "Shoulder to Shoulder" pattern, under the action of the core particle at 410 nm. (b) "Head-to-Head" pattern, under the action of the core particle at 650 nm wavelength.

The local field of the surface particles reciprocally impacts the local field of the core particle. The electric field distribution of the core particle, under the influence of the local field of the surface particles, is calculated using the FDTD method, and the results are presented in Figure 7. Figure 7(a) displays the electric field distribution of the core particle when the surface particles are in the "Shoulder to Shoulder" configuration, with an excitation wavelength of 410 nm. Influenced by the surface particles, the local field of the core particle is enhanced, especially in the gap between the particles. Figure 7(b) demonstrates the electric field distribution of the core particle when the surface particles are in a "Head-to-Head" arrangement, with an excitation wavelength of 650 nm. The most intense field of the core particle is primarily located in the outer area of the particle, due to the presence of the surface particles.

In comparison to the local field distribution of smooth spheres in the incident light, the local field of the flower-like silver particle is repositioned due to the surface particles and is significantly amplified in both the short and long wavelength ranges. This result aligns with our previous findings on flower-like silver particles [19,24].

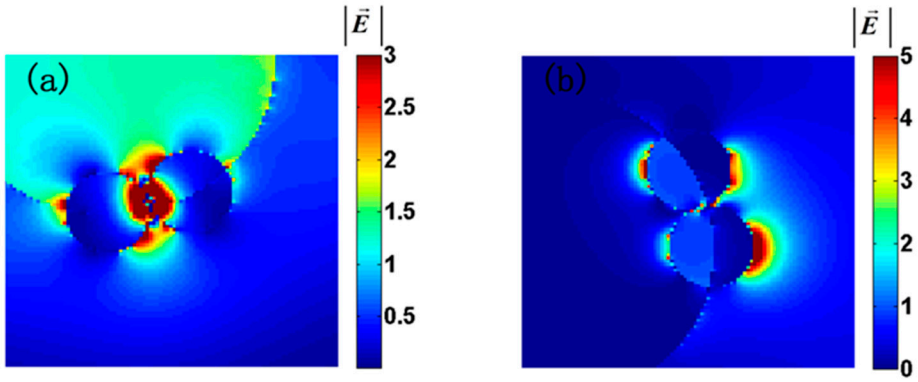

Figure 7. The electric field distribution of core particle under the effect of local field of surface particles. (a) at the wavelength of 410 nm, (b) at the wavelength of 650 nm.

The interaction between the surface particles and the core particles allows the flower-like silver particles to achieve a near-field enhancement across a broad spectrum. The field enhancement is defined as $|E|/|E_0|$ and is plotted as a function of wavelength in Figure 8. Here, $|E_0|$ is the incident field and $|E|$ is the maximum local field of the flower-like silver particle.

Figure 8 reveals that the field enhancement of the flower-like particle persists across a broad wavelength range of 400~800 nm, with the field enhancement being more significant in the shorter wavelength range. However, as the local field distribution is concentrated in the gap of the surface particles in the short wavelength range, the enhancement ratio of the spectral responsivity is conversely lower than in the long wavelength range.

Preprints (www.preprints.org) | NOT PEER-REVIEWED | Posted: 20 July 2023 doi:10.20944/preprints202307.1401.v1

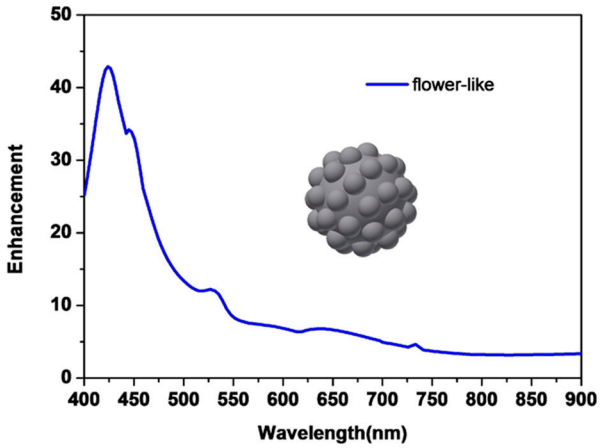

Figure 8. The local field enhancement $|E|/|E_0|$ of the flower-like silver particles to the wavelength.

After the incident light acts on the silver particles, due to the LSPR effect of the silver particles, the radiation field acting on the semiconductor is enhanced. After the semiconductor absorbs the photons, the internal electronic transition process can be explained by the perturbation theory in quantum mechanics [27,28]. According to Fermi's Golden Rule, the transition probability w_{if} of the semiconductor can be expressed as:

$$w_{if} = C\left|\vec{E}\right|^2 |M_{if}|^2 \quad (2)$$

where C is a constant, M_{if} represents the transition matrix element, $\vec{E}$ is the radiation field acting on the semiconductor. The relationship between the semiconductor's absorption coefficient α and the transition probability w_{if} can be expressed as:

$$\alpha \propto \sum w_{if} n_i n_f \quad (3)$$

where n_i and n_f represent the density of states of the semiconductor in the initial and final state respectively. According to equations (2) and (3), for amorphous silicon photovoltaic modules containing silver particles, the action of the silver particles enhances the radiation field acting on the semiconductor, thereby increasing the probability of internal electronic transitions in the semiconductor and raising the absorption coefficient. Generally speaking, for the same semiconductor, its absorption coefficient is a fixed value, but the introduction of silver particles can be expressed as an increase in its absorption coefficient. Thus, when light of the same intensity acts on amorphous silicon photovoltaic modules with and without silver particles, the photovoltaic modules containing silver particles have a larger absorption coefficient, therefore their light absorption is stronger, resulting in a larger photocurrent.

4. Conclusion

In summary, an a-Si p-i-n photovoltaic structure with flower-like silver particles deposited on the surface was fabricated. The transmittance, reflectance, and absorptance spectra measurements revealed that the absorption of this photovoltaic structure was enhanced in a broad wavelength range from 200 nm to 2000 nm by adding the flower-like silver particles on the surface. Furthermore, the spectral response of the a-Si p-i-n structure with and without silver particles respectively were measured at the wavelength range of 400~800 nm, which revealed that the maximum enhancement ratio of the responsivity can reach about 10, and the spectral response shape of composite structure was consistent with the structure without silver particles. The FDTD method was employed to investigate the mechanism. In our analysis, the sample was divided into two parts include the core particle and surface particles. We found that the interaction between the core particle and surface particles leads to the unique optical characteristics of the flower-like particles, which improved the performance of the a-Si p-i-n photovoltaic structure in a broadband range. Through these studies, we

demonstrate that, utilizing the subwavelength silver particles with roughness surface can achieve the spectral response of the photovoltaic modules enhanced in broadband range, which can improve the utilization efficiency of optical energy for the applications of sensing, imaging, optical communication, and energy harvesting. The theoretical analysis provides improved insight into the coupling of physical properties in photovoltaic modules incorporating metal particles.

Author Contributions: Y.W.: Methodology, Formal analysis, Date curation. F.Z.: Investigation, Software. X.F.: Funding acquisition, Writing—review & editing. Y.L.: Methodology, Data curation. C.W.: Investigation. X.H.: Software, Supervision. And L.Z.: Software, Funding acquisition. All authors have read and agreed to the published version of the manuscript.

Funding: This research was funded by the National Natural Science Foundation of China under Grant 61805178, and in part by the Natural Science Foundation of Shandong Provincial under Grant ZR2019MD011and ZR2020QA072.

Informed Consent Statement: Not applicable.

Data Availability Statement: Not applicable.

Conflicts of Interest: The authors declare no conflict of interest.

References

1. Wong, Joeson, S. T. Omelchenko , and H. A. Atwater. Impact of Semiconductor Band Tails and Band Filling on Photovoltaic Efficiency Limits. ACS ENERGY LETT **2021**, 6,52-57.
2. P. C. Harikesh, A. Surendran, B. Ghosh, R. A. John, A. Moorthy, N. Yantara, T. Salim, K. Thirumal, W. L. Leong and S. Mhaisalkar. Cubic NaSbS2 as an ionic–electronic coupled semiconductor for switchable photovoltaic and neuromorphic device applications. Adv. Mater **2020**, 32, 1906976.
3. Liu, Xu, S. Zhou. Progress on photovoltaic AlGaN photodiodes for solar-blind ultraviolet photodetection. CHIN OPT LETT **2022**, 20, 112501.
4. Yang, R., V. Van. Enhanced Small-Signal Responsivity in Silicon Microring Photodetector Based on Two-Photon Absorption. IEEE J SEL TOP QUANT **2020**, 26, 1-8.
5. Yang Xuxuan, L. Qu, F. Gao. High-Performance Broadband Photoelectrochemical Photodetectors Based on Ultrathin Bi2O2S Nanosheets. ACS APPL MATER INTER **2022**, 14, 7175-7183.
6. F. Cao, L. Meng, M. Wang, W. Tian, L. Li. Gradient energy band driven high-performance self-powered perovskite/CdS photodetector. Adv. Mater **2019,** 31, 1806725.
7. SB Liu， SJ Chang， SP Chang， CH Chen. An Amorphous (Al0.12Ga0.88)2O3 Deep Ultraviolet Photodetector. IEEE PHOTONICS J **2020**, 99, 1-1.
8. Dong Q., Wang F., Hu X., Lu Y., Zhao D., Zhang M. High-performance broadband photodetector based on PdSe2/black phosphorus heterodiode. APPL PHYS LETT **2022**, 120, 23.
9. Z. Zhong, Z. Xu, T. Sheng, J. Yao, W. Xing and Y. Wang. Unusual air filters with ultrahigh efficiency and antibacterial functionality enabled by ZnO nanorods. Acs. Appl. Mater. Inter **2015,** 7, 21538-21544.
10. Y. J. Kim, Y. J. Yoo, D. E. Yoo, D. W. Lee, M. S. Kim, H. J. Jang, Y.-C. Kim, J.-H. Jang, I. S. Kang, Y. M. Song. Enhanced light harvesting in photovoltaic devices using an edge-located one-dimensional grating polydimethylsiloxane membrane. Acs. Appl. Mater **2019**, 11, 36020-36026 .
11. Sun X, Y Su, Y Huang, J Tan. Photovoltaic Modules Monitoring Based on WSN With Improved Time Synchronization. IEEE Access **2019**, PP. 1-1.
12. P. Berini. Surface plasmon photodetectors and their applications. Laser. Photonics. Rev **2014**, 8, 197-220.
13. J.H. Zhong, J. Vogelsang, J.M. Yi, D. Wang, L. Wittenbecher, S. Mikaelsson, A. Korte, A. Chimeh, C. L. Arnold, P. Schaaf. Nonlinear plasmon-exciton coupling enhances sum-frequency generation from a hybrid metal/semiconductor nanostructure. Nat. Commun **2020**,11, 1-10.
14. M. Abbasi, C. I. Evans, L. Chen, D. Natelson. Single Metal Photodetectors Using Plasmonically-Active Asymmetric Gold Nanostructures. ACS. nano **2020**, 14, 17535-17542.
15. Wang, K., Niu, L., Tao, L., Zhang, Y., Zhou, X. Fabrication of tio_2 microspheres with continuously distributed sizes from nanometer to micronmeter: the increasing light scattering ability and the enhanced photovoltaic performance. SOL ENERGY **2021**, 11, 230.
16. A. Mondal, M. K. Yadav, S. Shringi, A. Bag. Extremely low dark current and detection range extension of Ga_2O_3 UV photodetector using Sn alloyed nanostructures. NANOTECHNOLOGY **2020**, 31, 294002.

17. M. W. Knight, H. Sobhani, P. Nordlander, N. J. Halas. Photodetection with active optical antennas. Science **2011**, 332, 702-704.
18. C.-S. Chang and L. J. Rothberg. Plasmon-enhanced photoconductivity in amorphous silicon thin films by use of thermally stable silica-coated gold nanorods. Chem. Mater **2015**, 27, 3211-3215.
19. F. Zhang, P. Chen, L. Zhang, S.-C. Mao, L. Lin, Y.-G. Tang, J.-C. Cui, X.-D. Qi, J.-H. Yang, Y.-F. Ma. Enhancement of Raman scattering by field superposition of rough submicrometer silver particles . Appl. Phys. Lett **2012**, 100, 173103.
20. H. Liang, Z. Li, W. Wang, Y. Wu, H. Xu. Highly surface-roughened "flower-like" silver nanoparticles for extremely sensitive substrates of surface-enhanced Raman scattering. Adv. Mater **2009**, 21, 4614-4618.
21. K. Kneipp, H. Kneipp, I. Itzkan, R. Dasari, M. S. Feld. Surface-enhanced Raman scattering and biophysics. J PHYS-CONDENS MAT **2002**, 14, 597-624.
22. Prucha E J , Palik E D. Handbook of optical constants of solids. Academic press, **1998.**
23. D. E. Carlson, C. R. Wronski. Amorphous silicon solar cell. Appl. Phys. Lett **1976**, 28, 671-673.
24. F. Zhang, P. Chen, X. Li, J. T. Liu, L. Lin, Z. W. Fan. Further localization of optical field for flower-like silver particles under laser radiation. Laser. Phys. Lett **2013**, 10, 045901.
25. L. Tong, H. Wei, S. Zhang, Z. Li, H. Xu. Optical properties of single coupled plasmonic nanoparticles. Phys. Chem. Chem. Phys **2013**,15, 4100-4109.
26. P. K. Jain, W. Huang, M. A. El-Sayed. On the universal scaling behavior of the distance decay of plasmon coupling in metal nanoparticle pairs: a plasmon ruler equation. Nano. Lett **2007**, 7, 2080-2088.
27. Fox M. Quantum Processes in Semiconductors, 5th edition[J]. Contemporary Physics, **2014**, 55(4): 338-339.
28. Cohen-Tannoudji C. Claude Cohen-Tannoudji; Bernard Diu; Franck Laloë: Quantenmechanik[M]. City: Walter de Gruyter, **2007**.